IEEE Access
Multidisciplinary ⋮ Rapid Review ⋮ Open Access Journal

Received 8 May 2023, accepted 30 May 2023, date of publication 9 June 2023, date of current version 26 June 2023.

Digital Object Identifier 10.1109/ACCESS.2023.3284558

RESEARCH ARTICLE

Wideband Matching Circuit for mmWave Series Fed Patch Array Antenna

MANOJ PRABHAKAR MOHAN[1], (Member, IEEE), JUAN MIGUEL JIMENO[2], SUN MEI[3], (Senior Member, IEEE), AROKIASWAMI ALPHONES[1], (Senior Member, IEEE), MOHAMMED YAKOOB SIYAL[1], (Senior Member, IEEE), AND MUHAMMAD FAEYZ KARIM[1], (Senior Member, IEEE)

[1]School of Electrical and Electronic Engineering, Nanyang Technological University, Singapore 639798
[2]NCS Corporation, Singapore 469272
[3]Institute of Microelectronics, Agency for Science, Technology and Research (A*STAR), Singapore 138634

Corresponding author: Muhammad Faeyz Karim (faeyz@ntu.edu.sg)

This work is funded by the Singapore Government through the Industry Alignment Fund - Industry Collaboration Projects Grant.

ABSTRACT A novel wide band matching circuit for the series fed patch array antenna at 80 GHz is proposed in this paper. The series fed patch array is designed with amplitude tapered configuration. First, the series fed patch array is matched using stub loaded transmission line (TL) with narrow band. Later, it is converted to wide band matching circuit using three quarter wave transformers and two half wavelength stubs. The sizes of these half wavelength stubs are reduced using the stub loaded and step impedance TLs. The simulated results of the series fed patch array with and without the connector are presented. The simulated −10 dB reflection coefficient bandwidth with connector is from 77.125 GHz to 83.95 GHz and the simulated co-polarized gain with connector is 13.73 dBi. The designed antenna array is fabricated along with the matching circuit and tested experimentally. The measured −10 dB reflection coefficient bandwidth is from 76.73 GHz to 86.08 GHz with the measured gain of the antenna is 13.3 dBi at 81.44 GHz.

INDEX TERMS mmWave, series fed patch antenna, stub loaded transmission line, wide bandwidth.

I. INTRODUCTION

Millimeter Wave bands have received a lot of attention recently due to their applications in 5G, IOT, level crossing monitoring and automotive radars [1], [2], [3]. The series fed patch array antennas has been used in many mmWave bands [4], [5], but one of the main disadvantages of these patch arrays is their narrow bandwidth behavior.

Therefore, several matching circuits have been designed to support wide band microstrip antennas. A series fed patch array with recessed microstrip feed for the terminal array element was proposed in [6]. Also, the width of the feed lines to other array elements are changed to match the impedance of the array elements. So, the bandwidth of 2.8% was achieved with better VSWR characteristic at 5 GHz. Two slits were made in the radiating edge opposite to feed of the patch element in [7] to increase the bandwidth of series fed array at *Ku* band. The bandwidth of the patch array was increased by using U-shaped slot in [8] with a thick substrate of 3.5mm thickness. The bandwidth of the patch antennas was reported to increase by using an E-shaped patch [9], half U-slot patch and half E-shaped patch [10] also. The probe feeding, air substrate and very thick substrate were used in [9] and [10].

A bandwidth of 8.4% was achieved for the patch antenna at 4.9 GHz by coupling two $\lambda/4$ resonators capacitively to the patch in [11]. A shorting pin was also used at the junction of two $\lambda/4$ resonators. The stacked patch configurations were also used to increase the impedance bandwidth [12], [13].

The bandwidth was increased by capacitively coupling the quarter wavelength short-circuited patch to the radiated edge of the main patch in [14]. Similarly, by capacitively coupling the resonators to the radiated edges [15], to non-radiated edges [16], and to the four edges [16] of the patch were used to increase the bandwidth. The bandwidth of the patch

The associate editor coordinating the review of this manuscript and approving it for publication was Fulvio Schettino.

at 40 GHz was increased by using slots and coupled feeding and the parasitic patches were used to reduce the directivity in [17]. The bandwidth of the antenna in [17] was further increased by using stubs in the matching circuit in [18]. This method of increasing the bandwidth by using the stubs in the matching circuit was initially proposed in [19]. Techniques like 3D printed curved patch [20], thin film multilayer antenna element [21] were reported to replace the conventional techniques like using thick substrates and multilayer printed circuit boards (PCBs) to improve the bandwidth of the antenna. The bandwidth of the antenna reported in [22], was increased by using stacked micro vias implemented by using new PCB technology called 'any layer PCB.'

Most of the techniques previously reported used slots to improve the bandwidth while other reported works in the literature used complex multi-layer PCBs. At 78.5 GHz the patch itself is so small and dimensions of the slots will become difficult to fabricate using current PCB fabrication technologies. Therefore, in this paper, the bandwidth of the series fed patch array is increased by using the stubs [19] in a single layer planar PCB configuration. The size of the stubs is further reduced by using stub loaded transmission lines (TLs) [23]. The stub loaded TL was reported to implement very high or low impedance TLs in Wilkinson power divider and to design compact Wilkinson power divider. Metamaterial [24], [25] has been used to reduce the size of the resonators. But this technique is not used in this paper, because metamaterial resonators at W band may become too small to fabricate using current fabrication technologies.

Impedance bandwidth of the series fed patch array is enhanced using the combined transformers and stub loaded TLs. The details about the design of the series fed patch array and the quarter wave matching circuit are discussed in section II along with the analysis of stub loaded TL. The design procedure of the wide band matching circuit along with the simulated results at each stage are discussed in section III. The simulated and measured results of the final design are also discussed in section III.

II. DESIGN OF SERIES FED PATCH ARRAY AND QUARTER WAVE TRANSFORMER

The conventional series fed patch array operating at mmWave frequency is shown in Fig. 1. The Dolph-Tschebyshev based amplitude tapering is used to design the three patches of the array and the distance between the patches is maintained at $\lambda/2$. In Fig. 1, the series fed patch array is shown without any matching circuit along with its simulated S-parameter response. The impedance of the series fed patch array is shown in Fig. 2. The impedance of the patch array is found from the reflection coefficient and the impedance of the feed line which is 50 Ω. First the series fed patch array is matched by using a quarter wave transformer as in Fig. 3. As shown in Fig. 3 the width of the quarter wave transformer is too small (0.06 mm) to fabricate using current fabrication techniques. The substrate used is Rogers 4350B with dielectric constant of 3.66, thickness of 0.168 mm and loss tangent of 0.0037.

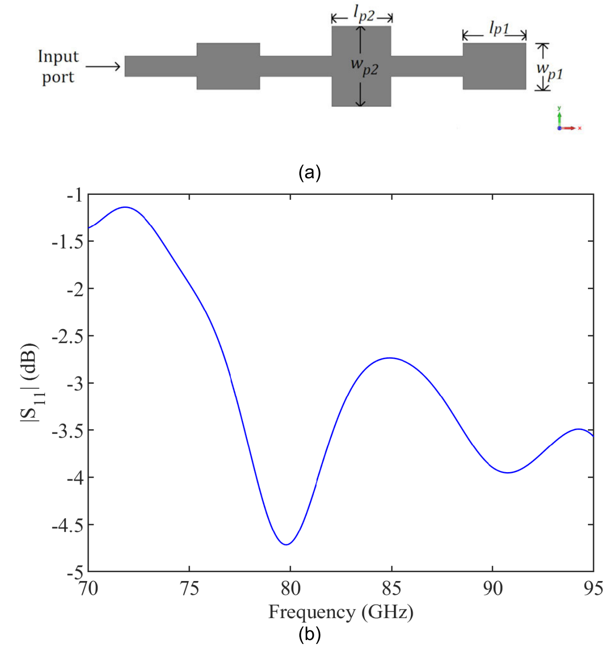

FIGURE 1. Conventional series fed patch array antenna with $w_{p1} = 0.72$mm, $l_{p1} = 0.98$mm, $w_{p2} = 1.25$mm, $l_{p2} = 0.92$mm (a) Structure of the series fed patch array with no matching circuit, and (b) simulated S parameter response.

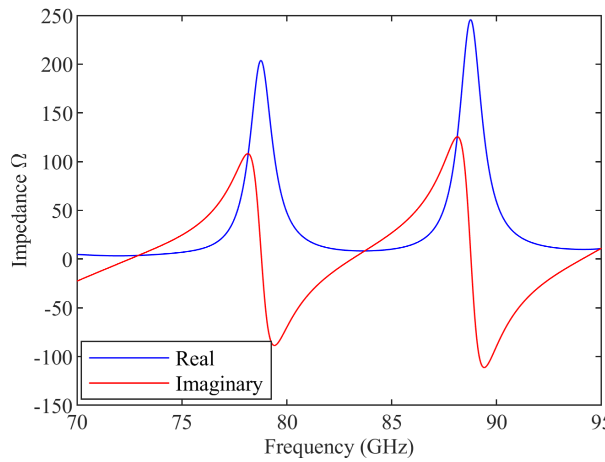

FIGURE 2. Impedance of the series antenna array.

In order to make the quarter wave transformer realizable, it is replaced by the stub loaded TL reported in [23]. The stub loaded TL has open or short-circuited stubs loaded at regular intervals, and it can be made equivalent to the conventional TLs. There is relatively a greater number of parameters in the stub loaded TL, so it gives more design freedom compared to conventional one. The conventional TL and the stub loaded TL are shown in Fig. 4. The ABCD matrices of the conventional TL [26] is given as

$$\begin{bmatrix} A & B \\ C & D \end{bmatrix} = \begin{bmatrix} \cos 2\theta_c & jZ_c \sin 2\theta_c \\ j\dfrac{\sin 2\theta_c}{Z_c} & \cos 2\theta_c \end{bmatrix} \tag{1}$$

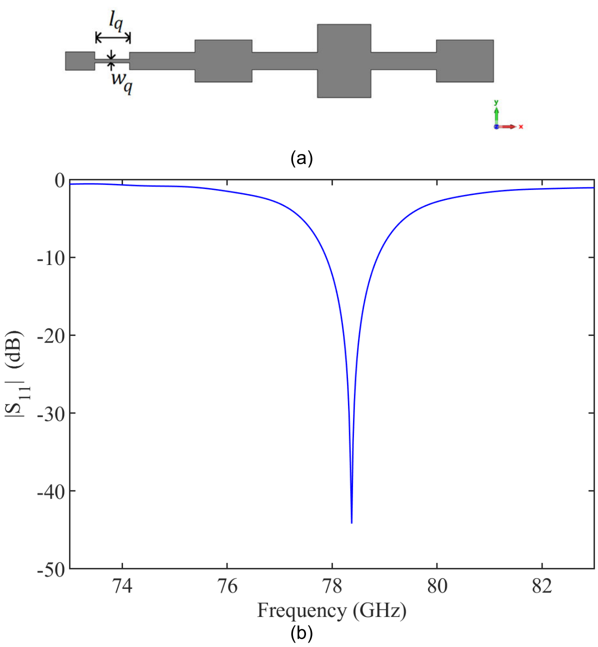

FIGURE 3. Series fed patch antenna matched by quarter wave transformer (a) structure with $w_q = 0.06$ mm, and $l_q = 0.6$ mm, and (b) simulated S parameter response.

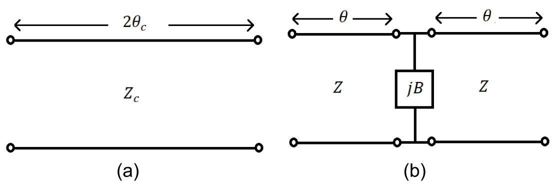

FIGURE 4. (a) Conventional TL, and (b) Stub loaded TL.

ABCD matrix of the stub loaded TL [21] is given as

$$\begin{bmatrix} A_T & B_T \\ C_T & D_T \end{bmatrix} = \begin{bmatrix} \cos 2\theta - \frac{ZB}{2}\sin 2\theta & jZ\sin 2\theta - jZ^2B\sin^2\theta \\ j\frac{\sin 2\theta}{Z} + jB\cos^2\theta & \cos 2\theta - \frac{ZB}{2}\sin 2\theta \end{bmatrix} \quad (2)$$

Equating (1) and (2) and simplifying, the following equations are obtained. The detailed derivation can be found in [27]

$$B = \sin 2\theta_c \cdot \left(\frac{Z^2 - Z_c^2}{Z_c \cdot Z^2}\right) \quad (3)$$

$$\tan\theta = \frac{Z_c}{Z}\tan\theta_c \quad (4)$$

For a chosen value of Z, the stub loaded TL parameters B and θ can be found from (3) and (4) from the conventional TL parameters Z_c and θ_c. In this case, quarter wave transformer is the conventional TL, and it is replaced with short-circuited stub loaded TL with low Z value so that it can be fabricated by current fabrication technologies. The series fed patch array matched by using short-circuited stub loaded TL is shown in Fig. 5 along with the photograph of the fabricated structure. The S-parameter response along with the simulated co-polarized radiation pattern in the XZ and YZ planes are also shown in Fig. 5. The Simulations

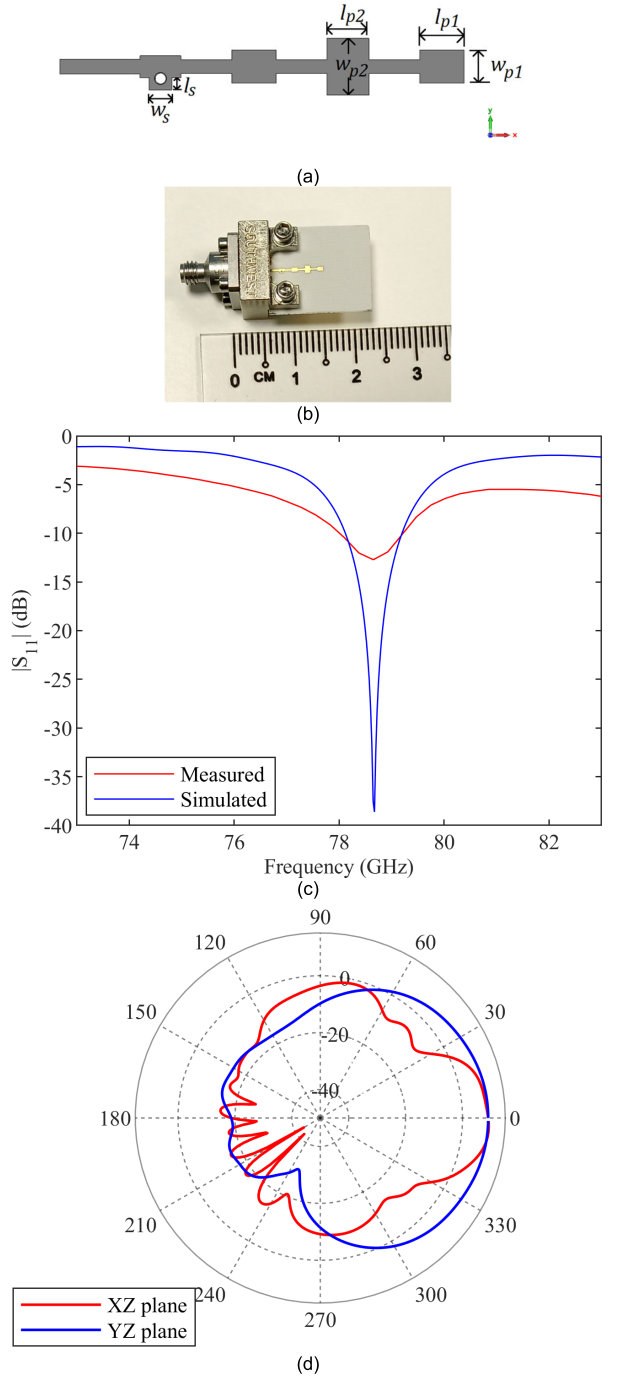

FIGURE 5. (a) Series fed patch array with stub loaded TL as quarter wave transformer with $w_{p1} = 0.72$mm, $l_{p1} = 0.98$mm, $w_{p2} = 1.25$mm, $l_{p2} = 0.92$mm, $w_s = 0.5$mm, and $l_s = 0.27$mm, (b) Photograph of the fabricated series fed patch array, (c) Measured and simulated S parameter response, and (d) Simulated Co-polarized radiation pattern in XZ plane and YZ plane.

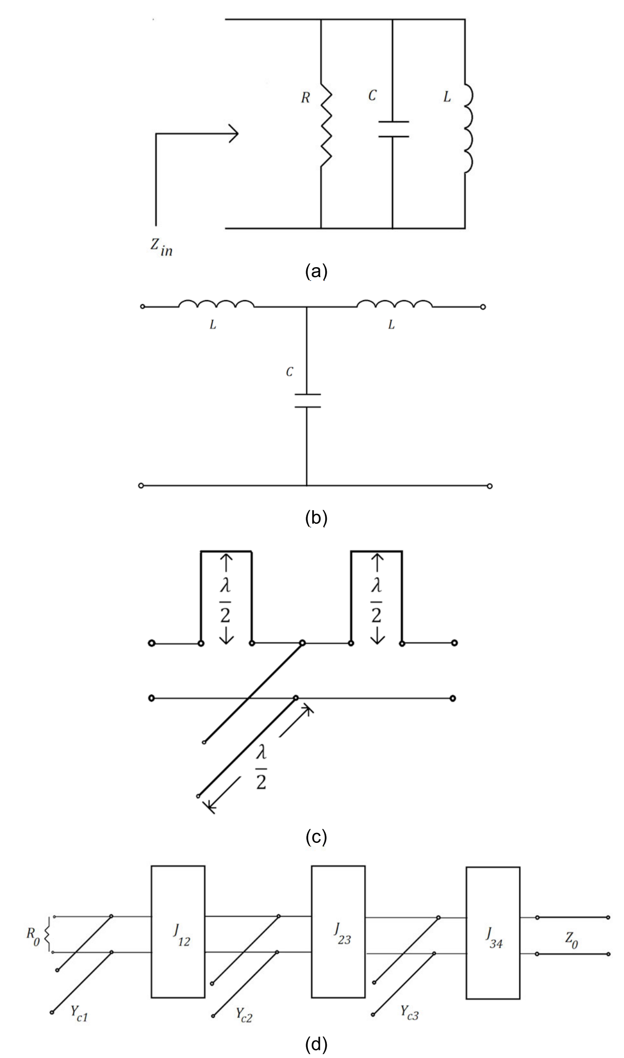

FIGURE 6. **(a) Equivalent circuit of the series fed patch array, (b) Circuit representing 3rd order low pass prototype, (c) Bandpass circuit formed from low pass circuit in (b), and (d) Final matching circuit with bandpass response.**

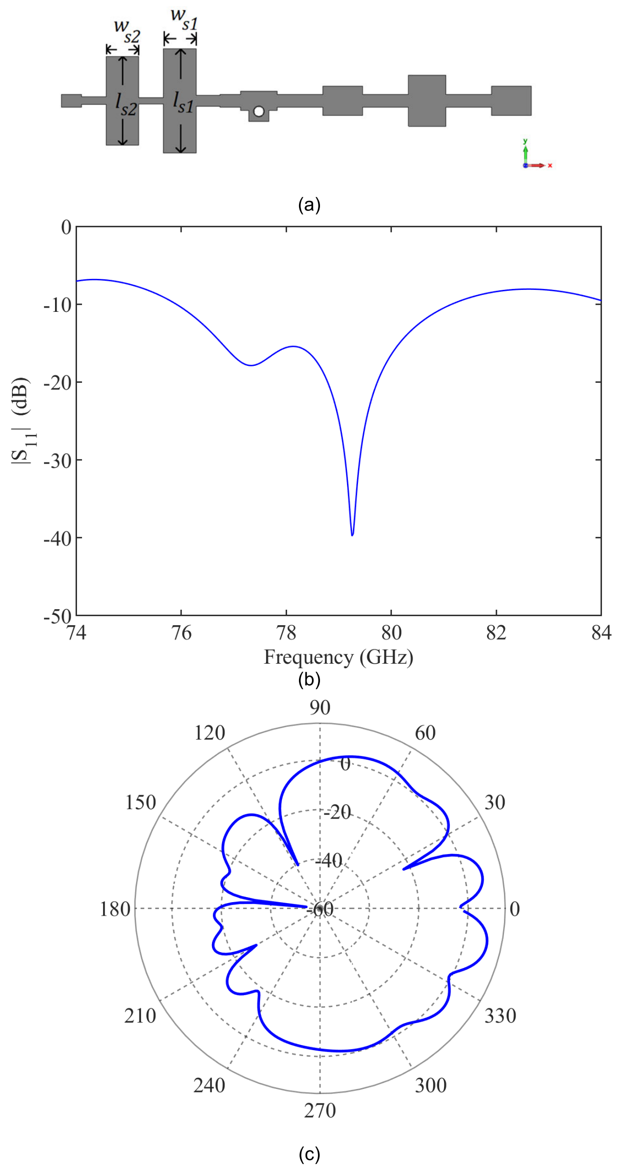

FIGURE 7. **(a) series fed patch array with wide band matching circuit, (b) Simulated S-parameter response with l_{s1} = 2.558 mm, w_{s1} = 0.8 mm, l_{s2} = 2.17mm, and w_{s2} = 0.8mm, and (c) Simulated co-polarized radiation pattern in XZ-plane.**

are done using CST Microwave Studio. The measured and simulated reflection coefficient of the antenna are −12.72 dB (78.65 GHz) and is −38.627 dB (78.675 GHz). The measured −10dB reflection coefficient bandwidth is from 78.01 GHz to 79.22 GHz whereas the simulated bandwidth is from 78.12 GHz to 79.2 GHz. The simulated gain of the antenna is 9.28 dB with polarization in X direction. The mismatch on reflection coefficient magnitude, and slight mismatch on the bandwidth, and frequency between the simulated and measured results are due to the fabrication errors and connector effects. The design of the proposed wide band matching circuit is explained in the following section.

III. DESIGN OF WIDE BANDWIDTH MATCHING CIRCUIT

In order to have the wide band matching, a reactive network consisting of three quarter wavelength TLs and two half wavelength stubs [19] are added to the narrow band series fed patch array (Fig. 5) as in Fig. 7. The equivalent circuit of the antenna is a parallel resonant circuit as shown in Fig. 6. The reactive network is implemented using the low pass prototype values. The third order low pass prototype is shown in Fig. 6 (b). This is converted to band pass resonant structure by replacing the parallel C by open circuited stubs and series L by short circuited stubs. Both the stubs are half wavelength in lengths. This circuit is shown in Fig. 6(c). The admittance inverters are used to convert the series short circuited half wavelength stubs to parallel open circuited half wavelength stubs. The final model is show in Fig. 6(d), where the parallel half wavelength stub Y_{c1} represents the parallel lossless resonant circuit of the antenna to be matched and the rest of the

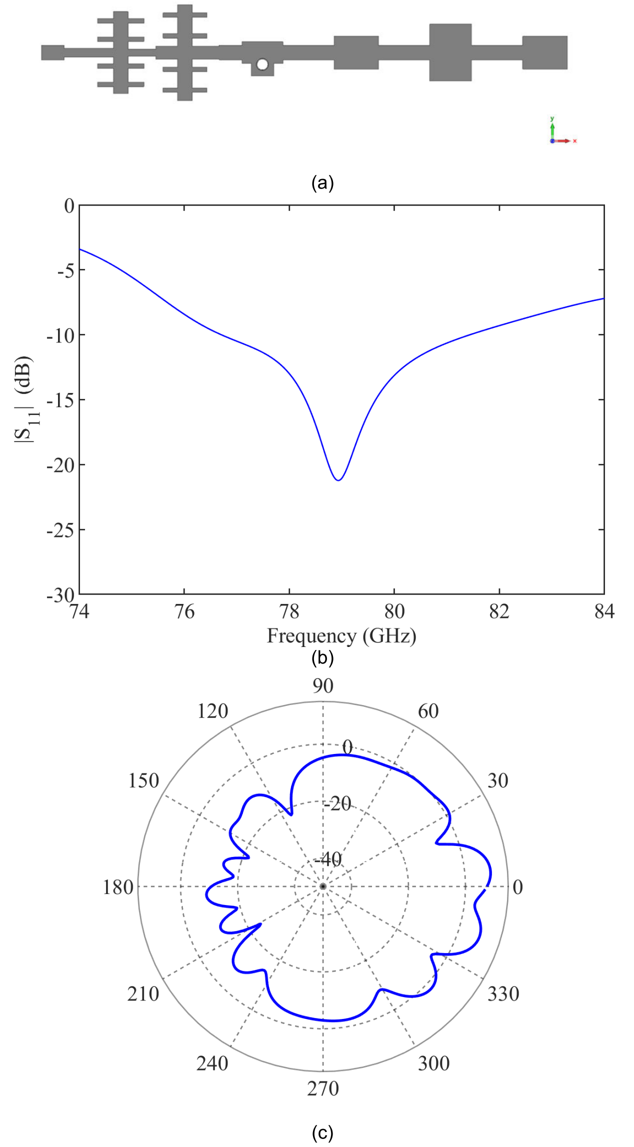

FIGURE 8. (a) series fed patch array with stub loaded TLs in the matching circuit, (b) Simulated S parameter response, and (c) Simulated co-polarized radiation pattern in XZ-plane.

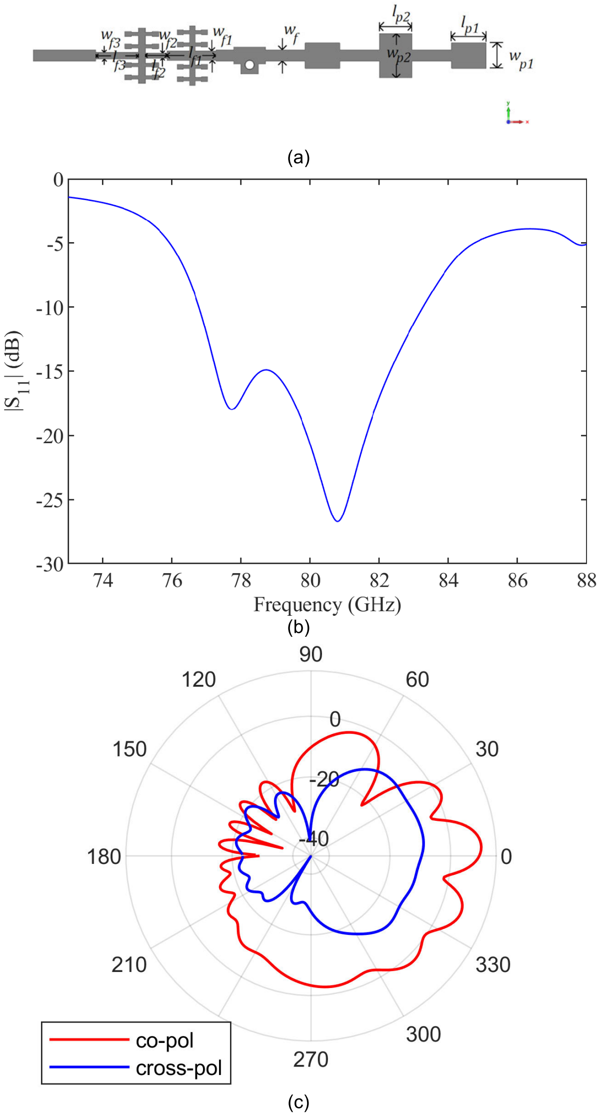

FIGURE 9. Series fed patch array (a) Structure with $w_{p1} = 0.72$mm, $l_{p1} = 0.98$mm, $w_{p2} = 1.25$mm, $l_{p2} = 0.92$mm, $w_f = 0.32$mm, $w_{f1} = 0.278$mm, $l_{f1} = 1.39$mm, $w_{f2} = 0.15$mm, $l_{f2} = 0.61$mm, $w_{f3} = 0.19$mm, and $l_{f3} = 1.2$mm, (b) Simulated S parameter response, and (c) Simulated Radiation pattern in XZ plane.

components are used to design the matching network. The design parameters of the quarter wavelength TLs, and half wavelength stubs are calculated using the equations.

$$J_{12} = \sqrt{\frac{\Lambda Y_{c2}}{R_0 g_2}} \tag{5}$$

$$J_{i,i+1} = \Lambda\sqrt{\frac{Y_{ci}Y_{ci+1}}{g_i g_{i+1}}}, \quad i = 2, 3, \ldots, n-1 \tag{6}$$

$$J_{n,n+1} = \sqrt{\frac{\Lambda Y_{cn}}{g_n g_{n+1} Z_0}} \tag{7}$$

$$Y_c^{i,i+1} = J_{i,i+1} \cos\left(\frac{\pi}{4}B\right) \tag{8}$$

where,

$$\Lambda = \tan\left(\frac{\pi}{2}B\right) \tag{9}$$

$$B = \frac{f_2 - f_1}{f_r} \tag{10}$$

and g_is are the low pass prototype values that can be found out from [28]. The parameters Y_{ci} give the admittances of the half wavelength stubs and $Y_c^{i,i+1}$ parameters give the admittances of the quarter wavelength TLs. The parametric values of Y_{ci} can be chosen arbitrary. The detailed explanation of the matching circuit can be found in [19]. In this case, $n = 3$ and 0.5 dB equal ripple low pass prototype values are

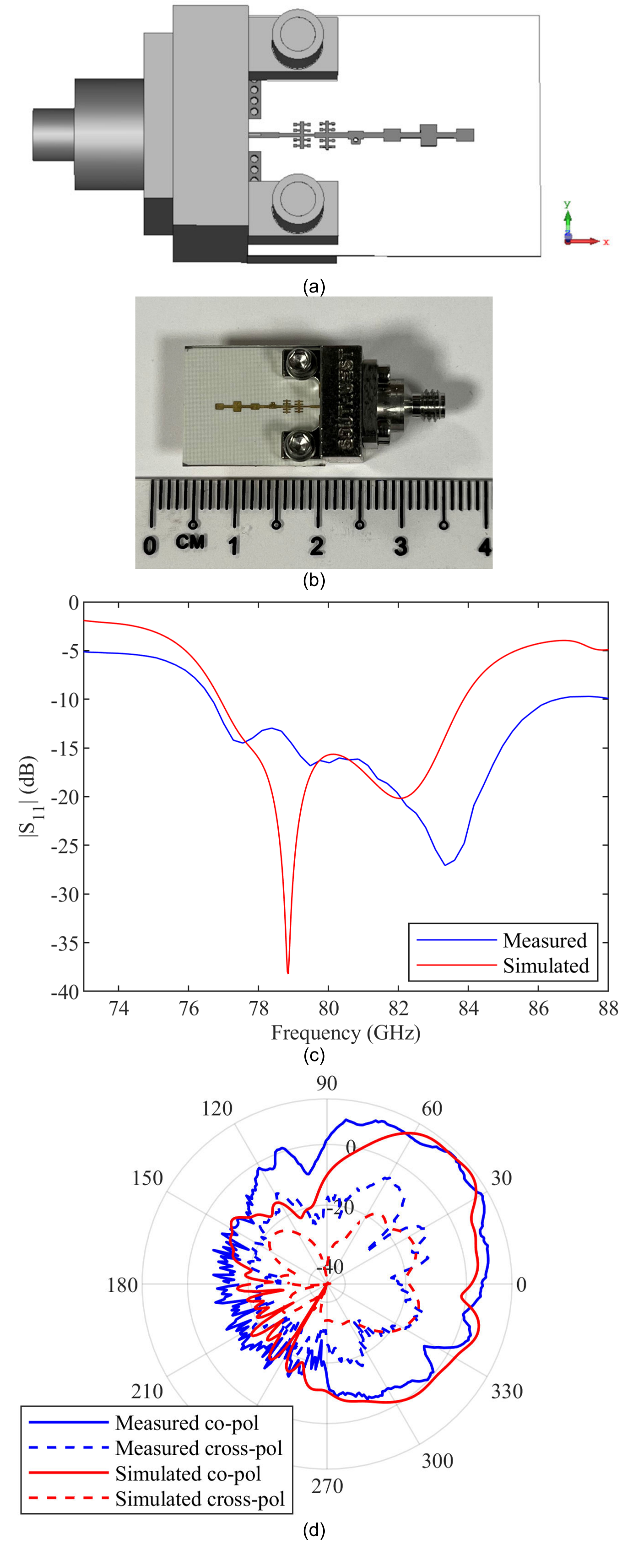

FIGURE 10. Proposed Series fed patch array with wide band characteristics (a) Structure with connector, (b) Photograph of the fabricated Series fed patch array with matching circuit, (c) S- parameter response with connector, and (d) Radiation pattern with connector in XZ plane.

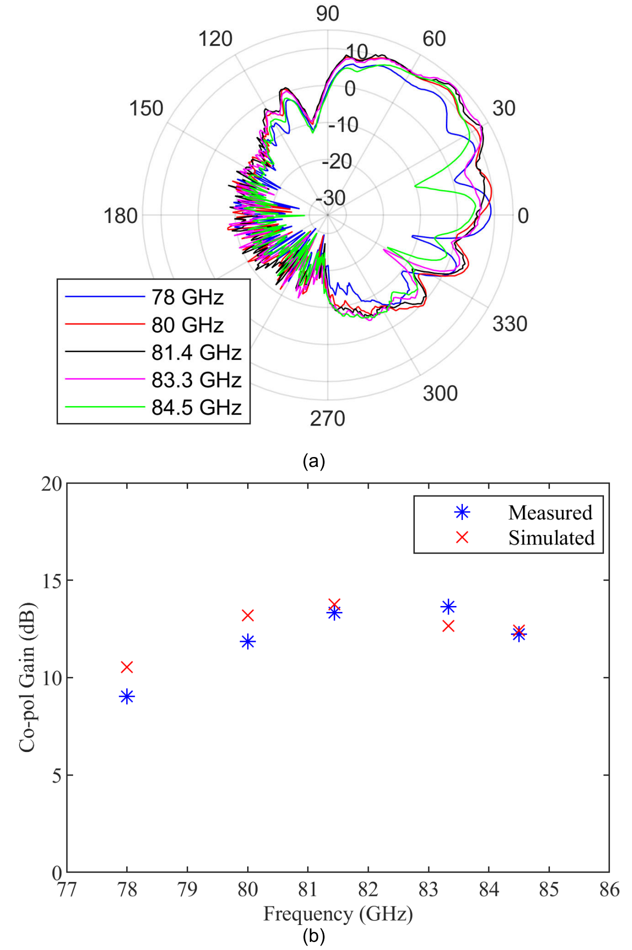

FIGURE 11. (a) Measured co-pol radiation pattern of the antenna at different frequencies, and (b) Measured and Simulated co-polarized gain of the antenna at different frequencies.

TABLE 1. Comparison of different stages of designed antenna.

	Bandwidth	Realized Gain (co-pol)	Largest dimension in matching circuit (mm)
Fig.5	1.37 %	9.28 dBi	0.5
Fig.7	6.68%	9dBi	2.558
Fig. 9	8.1%	10.28 dBi	1.39

chosen as g_i parameter values [28]. The values of Z_{ci}s are chosen as 12.5 Ω. Since the width of the stubs will be very wide at 12.5 Ω, two stubs with 25 Ω in parallel configuration are selected.

The structure of the wideband matching circuit and its simulated S-parameter response and the radiation pattern in XZ-plane are shown in Fig. 7. The simulated 10 dB bandwidth is from 75.904 GHz to 81.152 GHz (Fig.7(b)). The two half wavelength stubs are of comparable size to the patches. So, to reduce the size of the half wavelength stubs, the stub loaded TLs [23] are used. Two-unit cells of stub loaded TLs are used to implement each of the half wavelength stubs and it is shown in Fig. 8 along with the simulated S-parameter response and radiation pattern in XZ plane. The simulated 10 dB bandwidth from Fig. 8(b) is from 76.604 GHz to

TABLE 2. Comparison of the designed antenna with published works.

Reference	Frequency	Bandwidth	Antenna type	Technique
[5]	5 GHz	2.8%	Series fed patch array	Recessed feed on the last element
[10]	4.9 GHz	8.4%	Patch antenna	A pair of $\lambda/4$ resonators with shorting pin are gap coupled to patch
[18]	36.5 GHz	13.1%	Patch antenna	Slots in the patch + gap coupling + matching circuit from [19]
[20]	2.45	9%	Curved patch antenna	patch antenna over 3D printed cylindrical protrusion on substrate.
[21]	79 GHz	7.8% (SIW feed) 11.3% (GCPW and microstrip feed)	Grid array	Each antenna element is multilayered, achieved by thin films and is fed by SIW slots and parasitic elements on the top of the radiating element.
[22]	79	15% (impedance bandwidth)	Series fed patch array	stacked micro vias are implemented using 'any layer pcb' fabrication technology.
This work	80 GHz	11.49%	Series fed patch array	Matching circuit from [19] + stub loaded TL + stepped impedance TL

81.441 GHz. Even though the size of the matching circuit is reduced in Fig. 8(a) compared to Fig. 7(a) but still it can be reduced further. The TL of the stub loaded TL is replaced by a high impedance TL and the stubs of the stub loaded TL is replaced by using step impedance stubs [29] which reduces the size of the stubs. The final structure of the wide band series fed patch array is shown in Fig. 9. The simulated S parameter response along with the simulated radiation pattern is shown in Fig. 9. The comparison of the designed antenna in different stages is shown in Table 1 (only simulated values are used).

Since the connector is also in comparable size with the antenna in mmWave range of frequency, the antenna is simulated with connector as shown in Fig. 10. The photograph of the fabricated antenna is shown in Fig. 10 (b). The simulated S-parameter response with the connector along with the measured response are shown in Fig. 10(c). The simulated radiation pattern with connector along with the measured radiation pattern in XZ plane is shown in Fig. 10(d). The measured −10 dB reflection coefficient bandwidth of the series fed patch array with wide band matching circuit is from 76.73 GHz to 86.08 GHz. The simulated −10 dB reflection coefficient bandwidth is from 76.9 GHz to 83.85 GHz.

The radiation pattern is measured by connecting the antenna under test to the transmitter and WR-12 pyramidal horn antenna with 20 dBi typical gain is connected to the receiver. With the help of the rotor system connected to the receiver, the receiver horn antenna moves over the transmitter to find the radiation pattern. The measured co-polarized gain of the antenna at 81.44 GHz is 13.33 dBi and the simulated co-polarized gain with connector is 13.73 dBi. The antenna is polarized in X direction.

Comparing the simulated results of the antenna without and with connector shown in Fig. 9 and Fig. 10 respectively, the −10 dB reflection coefficient bandwidth is moved to higher frequency range from 76.78 GHz - 83.26 GHz to 76.9 GHz - 83.85 GHz. The simulated bandwidth is increased from 8.1% (Fig.9) to 8.647% (Fig.10) and to 11.49% in the measurement. The w band antennas in [21] and [22] also reported an increase in the measured impedance bandwidth compared to simulated ones. The maximum realized gain without the connector in Fig. 9 is 10.2 dBi (78.5 GHz) and it is increased to 13. 73 dBi (81.44 GHz) in the simulation with connector. The main lobe of the antenna is shifted from 3° (Fig.9) to 38° (Fig.10) and shifted to 45.4° in the measurement. The differences between the simulated and measured results are due to the fabrication tolerances and also the loss tangent used in the simulation was reported at 10 GHz. By using the loss tangent measured at 78.5 GHz and substrates with low conductive loss will help to reduce the difference between the simulated and measured results.

The measured co-pol radiation patterns of the antenna at different frequencies within the bandwidth are shown in Fig. 11 along with the measured and simulated co-pol gains at different frequencies within the band of interest. A detailed comparison of the designed antenna with the previously published works is shown in Table 2. In this work, the bandwidth of 11.49% at 80 GHz is achieved without using slots in the patch, gap coupling the feed, and multilayered PCB. In the future, the size of the matching circuit will be reduced further.

IV. CONCLUSION

A wide band matching circuit for a mmWave series fed patch array antenna with Dolph-Tschebyshev based amplitude tapering has been designed, fabricated, and validated experimentally. The measured −10 dB reflection coefficient bandwidth of the antenna is from 76.73 GHz to 86.08 GHz. The measured gain of the antenna is 13.3 dBi at 81.44 GHz. Proposed matching circuit configuration can be used for mmWave and microwave wireless system designs.

ACKNOWLEDGMENT

This research was conducted at Singtel Cognitive and Artificial Intelligence Lab for Enterprises (SCALE@NTU), which is a collaboration between Singapore Telecommunications Limited (Singtel) and Nanyang Technological University (NTU) that is funded by the Singapore Government through the Industry Alignment Fund - Industry Collaboration Projects Grant.

The authors would like to thank Dr. Nasimuddin from Institute of Infocomm Research I2R, Singapore, for his advice in improving the quality of the paper.

REFERENCES

[1] X. Lu, V. Petrov, D. Moltchanov, S. Andreev, T. Mahmoodi, and M. Dohler, ''5G-U: Conceptualizing integrated utilization of licensed and unlicensed spectrum for future IoT,'' *IEEE Commun. Mag.*, vol. 57, no. 7, pp. 92–98, Jul. 2019.

[2] A. Mazzinghi, A. Freni, A. Agostini, L. Bossio, and M. Albani, ''Industrial antenna development for 77-GHz level-crossing monitoring radar [antenna applications corner],'' *IEEE Antennas Propag. Mag.*, vol. 60, no. 5, pp. 95–106, Oct. 2018.

[3] W. A. Ahmad, M. Kucharski, A. Ergintav, H. J. Ng, and D. Kissinger, ''A planar differential wide fan-beam antenna array architecture: Modular high-gain array for 79-GHz multiple-input, multiple-output radar applications,'' *IEEE Antennas Propag. Mag.*, vol. 63, no. 4, pp. 21–32, Aug. 2021.

[4] J. Yan, H. Wang, J. Yin, C. Yu, and W. Hong, ''Planar series-fed antenna array for 77 GHz automotive radar,'' in *Proc. 6th Asia–Pacific Conf. Antennas Propag. (APCAP)*, Oct. 2017, pp. 1–3.

[5] T. Zalabsky, P. Bezousek, and D. Matousek, ''Patch antenna array for X-band FMCW sensor: An antenna system for detection of obstacles in near vicinity of a helicopter,'' in *Proc. Conf. Microw. Techn. (COMITE)*, Apr. 2015, pp. 1–5.

[6] T. Yuan, N. Yuan, and L.-W. Li, ''A novel series-fed taper antenna array design,'' *IEEE Antennas Wireless Propag. Lett.*, vol. 7, pp. 362–365, 2008.

[7] N. Boskovic, B. Jokanovic, M. Radovanovic, and N. S. Doncov, ''Novel *Ku*-band series-fed patch antenna array with enhanced impedance and radiation bandwidth,'' *IEEE Trans. Antennas Propag.*, vol. 66, no. 12, pp. 7041–7048, Dec. 2018.

[8] H. Wang, X. B. Huang, and D. G. Fang, ''A single layer wideband U-slot microstrip patch antenna array,'' *IEEE Antennas Wireless Propag. Lett.*, vol. 7, pp. 9–12, 2008.

[9] F. Yang, X.-X. Zhang, X. Ye, and Y. Rahmat-Samii, ''Wide-band E-shaped patch antennas for wireless communications,'' *IEEE Trans. Antennas Propag.*, vol. 49, no. 7, pp. 1094–1100, Jul. 2001.

[10] R. Chair, C.-L. Mak, K.-F. Lee, K.-M. Luk, and A. A. Kishk, ''Miniature wide-band half U-slot and half E-shaped patch antennas,'' *IEEE Trans. Antennas Propag.*, vol. 53, no. 8, pp. 2645–2652, Aug. 2005.

[11] J. Zhang, L. Zhu, Q. Wu, N. Liu, and W. Wu, ''A compact microstrip-fed patch antenna with enhanced bandwidth and harmonic suppression,'' *IEEE Trans. Antennas Propag.*, vol. 64, no. 12, pp. 5030–5037, Dec. 2016.

[12] R. B. Waterhouse, ''Stacked patches using high and low dielectric constant material combinations,'' *IEEE Trans. Antennas Propag.*, vol. 47, no. 12, pp. 1767–1771, Dec. 1999.

[13] S. D. Targonski, R. B. Waterhouse, and D. M. Pozar, ''Design of wide-band aperture-stacked patch microstrip antennas,'' *IEEE Trans. Antennas Propag.*, vol. 46, no. 9, pp. 1245–1251, Sep. 1998.

[14] C. Wood, ''Improved bandwidth of microstrip antennas using parasitic elements,'' *IEE Proc. H, Microw. Opt. Antennas*, vol. 127, no. 4, pp. 231–234, Aug. 1980.

[15] G. Kumar and K. Gupta, ''Broad-band microstrip antennas using additional resonators gap-coupled to the radiating edges,'' *IEEE Trans. Antennas Propag.*, vol. AP-32, no. 12, pp. 1375–1379, Dec. 1984.

[16] G. Kumar and K. Gupta, ''Nonradiating edges and four edges gap-coupled multiple resonator broad-band microstrip antennas,'' *IEEE Trans. Antennas Propag.*, vol. AP-33, no. 2, pp. 173–178, Feb. 1985.

[17] K. Wang, J. Kornprobst, and T. F. Eibert, ''Microstrip fed broadband mm-wave patch antenna for mobile applications,'' in *Proc. IEEE Int. Symp. Antennas Propag. (APSURSI)*, Jul. 2016, pp. 1637–1638.

[18] J. Kornprobst, K. Wang, G. Hamberger, and T. F. Eibert, ''A mm-wave patch antenna with broad bandwidth and a wide angular range,'' *IEEE Trans. Antennas Propag.*, vol. 65, no. 8, pp. 4293–4298, Aug. 2017.

[19] H. F. Pues and A. R. Van de Capelle, ''An impedance-matching technique for increasing the bandwidth of microstrip antennas,'' *IEEE Trans. Antennas Propag.*, vol. 37, no. 11, pp. 1345–1354, Nov. 1989.

[20] G. Muntoni, G. Montisci, G. A. Casula, F. P. Chietera, A. Michel, R. Colella, L. Catarinucci, and G. Mazzarella, ''A curved 3-D printed microstrip patch antenna layout for bandwidth enhancement and size reduction,'' *IEEE Antennas Wireless Propag. Lett.*, vol. 19, no. 7, pp. 1118–1122, Jul. 2020.

[21] O. Khan, J. Meyer, K. Baur, and C. Waldschmidt, ''Hybrid thin film antenna for automotive radar at 79 GHz,'' *IEEE Trans. Antennas Propag.*, vol. 65, no. 10, pp. 5076–5085, Oct. 2017.

[22] H. Aliakbari, M. Mosalanejad, C. Soens, G. A. E. Vandenbosch, and B. K. Lau, ''79 GHz multilayer series-fed patch antenna array with stacked micro-via loading,'' *IEEE Antennas Wireless Propag. Lett.*, vol. 21, no. 10, pp. 1990–1994, Oct. 2022.

[23] J.-L. Li and B.-Z. Wang, ''Novel design of Wilkinson power dividers with arbitrary power division ratios,'' *IEEE Trans. Ind. Electron.*, vol. 58, no. 6, pp. 2541–2546, Jun. 2011.

[24] N. Mishra and R. K. Chaudhary, ''A compact CPW fed CRR loaded four element metamaterial array antenna for wireless application,'' *Prog. Electromagn. Res.*, vol. 159, pp. 15–26, 2017.

[25] D. Sarkar, K. Saurav, and K. V. Srivastava, ''Four-element array of complementary split-ring resonator loaded printed directive dipoles for triple band applications,'' *Electron. Lett.*, vol. 52, no. 10, pp. 785–786, May 2016.

[26] D. M. Pozar, *Microwave Engineering*, 4th ed. Hoboken, NJ, USA: Wiley, 2012.

[27] M. P. Mohan, L. Zhao, J. Jimeno, A. Alphones, M. Y. Siyal, and M. F. Karim, ''Design of stub loaded transmission line matching circuit for series fed patch array,'' in *Proc. IEEE Int. Symp. Antennas Propag. USNC-URSI Radio Sci. Meeting (APS/URSI)*, Dec. 2021, pp. 1279–1280.

[28] L. G. Matthaei, L. Young, and E. M. T. Jones, *Microwave Filters Impedance-Matching Networks and Coupling Structure*. Dedham, MA, USA: Artech House, 1980.

[29] M. Sagawa, M. Makimoto, and S. Yamashita, ''Geometrical structures and fundamental characteristics of microwave stepped-impedance resonators,'' *IEEE Trans. Microw. Theory Techn.*, vol. 45, no. 7, pp. 1078–1085, Jul. 1997.

MANOJ PRABHAKAR MOHAN (Member, IEEE) received the Ph.D. degree from the School of Electrical and Electronics Engineering, Nanyang Technological University, Singapore, in 2019. He was a Research Associate with Nanyang Technological University, where he has been a Research Fellow, since 2019. His research interest includes the design of passive microwave circuits like filters, antennas, and metasurfaces.

JUAN MIGUEL JIMENO received the B.S. degree from the Don Bosco Technical College, Philippines, in 2013. Since 2014, he has been involved in autonomous systems. He has also been involved in government-related robotics projects in Singapore, where he led the development of last mile delivery drones for Singapore Post, and the Self Driving Wheelchair which piloted in Changi General Hospital. He is currently involved in applied robot learning research with NCS Corporation, Singapore. His research interest includes machine learning and controls.

SUN MEI (Senior Member, IEEE) received the B.E. degree in electronic engineering from Hunan University, China, in 2000, the M.E. degree in electronic engineering from the Beijing Institute of Technology, China, in 2003, and the Ph.D. degree in electronic engineering from Nanyang Technological University (NTU), Singapore, in 2007. She became a Research Associate with NTU, in 2006, and subsequently converted to a Research Fellow, in 2007. She joined the Institute for Infocomm Research, in 2009, and the Institute of Microelectronics, in 2019, as a Scientist, under the Agency for Science, Technology and Research (A*STAR), Singapore. She has filled four U.S. patents and authored one book chapter and more than 70 technical papers in refereed journals and conference proceedings. Her research interests include millimeter-wave beamforming systems/antenna in package for 5G, SOTM, 60 GHz, and 77 GHz autonomous car radar applications. In 2013, she was elected as a Senior Member of IEEE with a contribution to millimeter-wave Antenna in Package (AiP) technology. She was a recipient of the 2012 S. A. Schelkunoff Prize Paper Award from the IEEE Antennas and Propagation Society and the Best Paper Award from the IEEE IWAT 2007 Conference. She has been serving as the Vice Chair for the IEEE Singapore RFID Chapter and the Publication Chair for the IEEE SOLI 2018 Conference.

AROKIASWAMI ALPHONES (Senior Member, IEEE) received the B.Tech. degree from the Madras Institute of Technology, in 1982, the M.Tech. degree from the Indian Institute of Technology Kharagpur, in 1984, and the Ph.D. degree in optically controlled millimeter wave circuits from the Kyoto Institute of Technology, Japan, in 1992. From 1996 to 1997, he was a JSPS Visiting Fellow in Japan. From 1997 to 2001, he was with the Centre for Wireless Communications, National University of Singapore, where he was involved in the research on optically controlled passive/active devices. Since 2001, he has been with the School of Electrical and Electronic Engineering, Nanyang Technological University, Singapore. He has 35 years of research experience. He has published and presented more than 320 technical papers in peer-reviewed international journals/conferences. His current interests include electro-magnetic analysis on planar RF circuits and integrated optics, microwave photonics, visible light communication and positioning, metamaterial-based leaky wave antennas, and wireless power transfer technologies. He was involved many IEEE flagship conferences held in Singapore and the General Chair of APMC 2009, MWP 2011, TENCON 2016, and APMC 2019. He was the Chairperson of the IEEE Singapore Section, from 2015 to 2016 and 2018. He is a Singapore Representative of IEICE, Japan, and a Panel Member of the IEEE Conference Application Review Committee.

MOHAMMED YAKOOB SIYAL (Senior Member, IEEE) received the M.Sc. and Ph.D. degrees in computer engineering from The University of Manchester, U.K., and the M.B.A. degree (specializing in IT) from the European Management School, Surrey University, U.K. He has been with Universities in Europe and Asia, and also involved in teaching, research, and supervising/advising students in cyber security areas with the School of Electrical and Electronic Engineering, NTU, Singapore. With his inter-disciplinary background, he has been teaching and conducting research in information security, medical image processing, computer vision, e-business/IT management, innovation, and technology management areas. He has also conducted several research projects on ''biometric-based'' cyber security. He has been conducting short courses and seminars on E-commerce, blockchain technology, Industry 4.0 and cyber security threats, AI and big data, innovation and technology management, innovative business models, cloud computing and big data, and sustainable smart cities. He has also been conducting short courses on cyber security under skills future in Singapore for many years and so far, he has successfully conducted more than 25 courses, and teaching cyber security and information security courses with NTU for many years. He has published 230 refereed journal and conference papers and has authored eight books. At NTU, he has won numerous teaching awards, including the Best Dressed Teacher, the Teaching Excellence Award, and the Nanyang Teaching Excellence Award. He was also a National Day Award recipients, in 2018.

MUHAMMAD FAEYZ KARIM (Senior Member, IEEE) received the B.Eng. degree from the National University of Sciences and Technology (NUST), the M.Sc. and Ph.D. degrees from Nanyang Technological University (NTU), Singapore, and the M.B.A. degree from Lancaster University, U.K.

Before joining NTU, he worked as the Deputy Department Head/Project Manager/Research Scientist with the Institute for Infocomm Research (I2R), A*STAR, from 2007 to 2017. From 2009 to 2017, he also held concurrent appointment as an Adjunct Assistant Professor with the National University of Singapore, (NUS). He worked as a Test Engineer with Emerson Process Management, a US MNC and prior to that employed as a Research Associate/RF Engineer with NTU. He is the Co-Founder of a spinoff company, Wavescan Technologies Pte. Ltd. He has published more than 80 scientific journal and conference papers. He coauthored a book on RF MEMS switches and integrated switching circuits. His research interests include active/passive millimeter wave radar sensing and imaging, quantum optics and engineering, silicon photonics, wireless power transfer and harvesting, chipless RFID, tunable and reconfigurable circuits, and passive microwave and millimeter components and modules.

Dr. Karim was a part of the committee involved in organizing international technical conferences, like IEEE APMC 2019, IEEE AWPT 2017, IEEE TENCON 2016, IEEE IMWS Conference 2013 and Microwave Photonics Conference (MWP), Singapore, in 2011. He is the Chair of the IEEE Singapore Section.